European Journal of Radiology 82 (2013) 1539–1545

Contents lists available at SciVerse ScienceDirect

European Journal of Radiology

journal homepage: www.elsevier.com/locate/ejrad

Detecting subarachnoid hemorrhage: Comparison of combined FLAIR/SWI versus CT

Rajeev Kumar Verma [a,*], Raimund Kottke [a,1], Lukas Andereggen [b,1], Christian Weisstanner [a,1], Christoph Zubler [a,1], Jan Gralla [a,1], Claus Kiefer [a,1], Johannes Slotboom [a,1], Roland Wiest [a,1], Gerhard Schroth [a,1], Christoph Ozdoba [a,1], Marwan El-Koussy [a,c,1]

[a] University Institute of Diagnostic and Interventional Neuroradiology, Support Center for Advanced Neuroimaging, University of Bern, Inselspital, Freiburgstrasse 4, 3010 Bern, Switzerland
[b] Department of Neurosurgery, University of Bern, Inselspital, Freiburgstrasse 4, 3010 Bern, Switzerland
[c] Department of Radiology, Cairo University Hospitals, 1 KasrEleini Street, 11461 Cairo, Egypt

ARTICLE INFO

Article history:
Received 17 December 2012
Received in revised form 22 March 2013
Accepted 26 March 2013

Keywords:
Subarachnoid hemorrhage
Computer tomography
Magnet resonance imaging
Susceptibility weighted imaging
Intracranial hemorrhage

ABSTRACT

Objectives: Aim of this study was to compare the utility of susceptibility weighted imaging (SWI) with the established diagnostic techniques CT and fluid attenuated inversion recovery (FLAIR) in their detecting capacity of subarachnoid hemorrhage (SAH), and further to compare the combined SWI/FLAIR MRI data with CT to evaluate whether MRI is more accurate than CT.
Methods: Twenty-five patients with acute SAH underwent CT and MRI within 6 days after symptom onset. Underlying pathology for SAH was head trauma ($n=9$), ruptured aneurysm ($n=6$), ruptured arteriovenous malformation ($n=2$), and spontaneous bleeding ($n=8$). SWI, FLAIR, and CT data were analyzed. The anatomical distribution of SAH was subdivided into 8 subarachnoid regions with three peripheral cisterns (frontal-parietal, temporal-occipital, sylvian), two central cisterns and spaces (interhemispheric, intraventricular), and the perimesencephalic, posterior fossa, superior cerebellar cisterns.
Results: SAH was detected in a total of 146 subarachnoid regions. CT identified 110 (75.3%), FLAIR 127 (87%), and SWI 129 (88.4%) involved regions. Combined FLAIR and SWI identified all 146 detectable regions (100%). FLAIR was sensitive for frontal-parietal, temporal-occipital and Sylvian cistern SAH, while SWI was particularly sensitive for interhemispheric and intraventricular hemorrhage.
Conclusions: By combining SWI and FLAIR, MRI yields a distinctly higher detection rate for SAH than CT alone, particularly due to their complementary detection characteristics in different anatomical regions. Detection strength of SWI is high in central areas, whereas FLAIR shows a better detection rate in peripheral areas.

1. Introduction

Computed tomography (CT) is the preferred method for routine imaging of patients with suspected subarachnoid hemorrhage (SAH) due to its high sensitivity and wide availability [1,2]. Until recently, MRI was thought to be less sensitive for detection of SAH. However, recent studies have demonstrated that fluid attenuated inversion recovery (FLAIR) MRI is equal to or even more sensitive than CT for detection of acute or subacute SAH [3–5]. Both methods have their limitations; CT has a lower sensitivity in the posterior fossa due to beam-hardening artifacts, whereas cerebrospinal fluid (CSF) pulsations, vascular pulsation or supplemental oxygen may cause FLAIR artifacts in the form of hyperintense signal of the subarachnoid spaces [4–7].

Susceptibility weighted imaging (SWI) is extremely sensitive for susceptibility dephasing from deoxyhemoglobin, hemosiderin, iron and calcium. Hence, SWI is considered to be a sensitive method for the identification of intracranial hemorrhage [8–10]. Recent work from Wu et al. highlighted the utility of SWI in cases with traumatic SAH [11]. The aim of this study is to make a step further.

* Corresponding author at: University Institute of Diagnostic and Interventional Neuroradiology, Support Center for Advanced Neuroimaging, Freiburgstrasse 4, 3010 Bern, Switzerland. Tel.: +41 31 6322655, fax: +41 31 6324872.
E-mail addresses: rajeev.verma@insel.ch, verma@gmx.ch (R.K. Verma), raimund.kottke@insel.ch (R. Kottke), lukas.andereggen@insel.ch (L. Andereggen), christian.weisstanner@insel.ch (C. Weisstanner), christoph.zubler@insel.ch (C. Zubler), jan.gralla@insel.ch (J. Gralla), claus.kiefer@insel.ch (C. Kiefer), johannes.slotboom@insel.ch (J. Slotboom), roland.wiest@insel.ch (R. Wiest), gerhard.schroth@insel.ch (G. Schroth), christoph.ozdoba@insel.ch (C. Ozdoba), Marwan.el-koussy@insel.ch (M. El-Koussy).
[1] Tel.: +41 31 6322655.

0720-048X/$ – see front matter © 2013 Elsevier Ireland Ltd. All rights reserved.
http://dx.doi.org/10.1016/j.ejrad.2013.03.021

We hypothesized that a combination of FLAIR and SWI would improve the detection rate compared to CT alone in acute SAH. Another objective is to compare SWI alone with the established methods, FLAIR and CT, in SAH. To our best knowledge, no study has yet compared FLAIR and SWI regarding their differing capacities for detecting SAH in diverse anatomical areas of subarachnoid space, or investigated whether SWI can provide additional information.

2. Materials and methods

2.1. Patient data

For this retrospective study, we examined patients with acute SAH admitted to our institution from July 2010 to November 2011. Patients were included if they underwent CT and MRI within 6 days after symptom onset. A total of 25 patients (8 women, 17 men; age range, 13–80 years; mean age, 48.1 years) fulfilled the inclusion criteria (Table 1). Based on the clinical and imaging assessment, the causes of SAH were head trauma ($n = 9$), ruptured aneurysm ($n = 6$), ruptured arteriovenous malformation (AVM) ($n = 2$), or bleeding of unknown origin ($n = 8$) in which patients suffered an acute onset of severe headache without trauma. SAH was diagnosed by cross section imaging initially, either with CT or MRI. According to the routine diagnostic protocols in our institution the aneurysms, vascular malformations and SAH of unknown cause were further investigated by digital subtraction angiography in all 16 non-trauma patients to clarify the etiology of SAH and intervention if necessary. In those 8 patients with still unknown cause for SAH, 2 had anticoagulant therapy and 2 had antiplatelet therapy. In 5 of them SAH was clearly detectable SAH in MRI and CT. The remaining 3 patients underwent lumbar puncture – performed after the CT and MRI investigations – and SAH was confirmed. 22 patients underwent CT scan on the day of symptom onset, 2 on the second day and one on the third day (mean for all 25 patients 6:18 h after clinical onset). Nine patients underwent MRI on the same day, 5 on the second, one on the third, 3 on the fourth and 7 on the fifth day after clinical onset (mean 54:16 h after onset). Fisher grade classification in all patients was determined for each modality, average Fisher grade was calculated. Since the data was neither normally distributed nor interval or ratio scaled the sign test was chosen. After applying a Bonferroni correction (three in this case) none of the test statistics were found to be significant. Patients with trauma or ruptured AVM who showed parenchymal hemorrhage close to the SAH were excluded from the study to avoid blooming effects.

Consent from the patient or, if the patient was not able to sign, from a family member was obtained after ruling out contraindications for MRI and before MRI scan. The study was approved by the local ethics committee.

2.2. MR and CT imaging

18 patients were examined in a 1.5 T Magnetom Avanto MRI scanner and 7 patients in a clinical 3 T Magnetom Verio MR system (Siemens Healthcare, Erlangen, Germany) using a 12-channel or 32-channel head coil, respectively. FLAIR sequences in the coronal plane were acquired with TR/TE 8500/81 (8500/81 at 3 T), slice thickness = 4 mm, and field of view (FOV) = 220 mm. Axial SWI sequences at 1.5 T: TR/TE = 49/40 ms, FOV = 230 mm, matrix size 320×208, voxel size 0.9 mm × 0.7 mm × 1.8 mm, flip angle = 15°; SWI at 3 T TR/TE = 28/20 ms, FOV = 230 mm, matrix = 320×168, voxel size 1.0 mm × 0.7 mm × 1.2 mm, flip angle 15°.

Sequential CT scans of the brain were performed on two CT scanners: A GE Lightspeed 8-row detector scanner (GE Healthcare, Milwaukee, Wisconsin, USA): tube current = 180 mA, kvp = 120 kV, standard kernel, slice thickness 2.5 mm/1.25 mm (supratentorial/infratentorial), and FOV = 220 mm (7 examinations), and a Somatom S16 scanner (Siemens Healthcare, Erlangen, Germany): tube current = 200–220 mA, kvp = 120 kV, convolution kernel H41s, slice thickness 1.5 mm, and FOV 220 mm (18 examinations).

2.3. Image analysis

For categorizing the subarachnoid space we used the method described by Wu et al., who divided the subarachnoid space into 8 distinct anatomical regions [11]. This method offers a

Table 1
Clinical demographics and Fisher grade classification.

Patient	Gend/Age	Cause of SAH	Time between symptom onset and CT	Time between symptom onset and MRI	Fisher grade classification in CT	Fisher grade classification in FLAIR	Fisher grade classification in SWI
1	M/48	Trauma	6:00 h	2:20 h	4	4	4
2	F/53	Unknown	3:50 h	41:00 h	3	3	3
3	M/47	Aneurysm	16:20 h	41:30 h	3	3	4
4	M/47	Unknown	9:00 h	99:40 h	2	2	2
5	F/53	Aneurysm	47:20 h	46:20 h	4	4	4
6	M/57	Unknown	1:30 h	8:00 h	3	3	4
7	F/44	Trauma	2:40 h	30:10 h	2	2	4
8	M/22	Trauma	1:10 h	82:10 h	2	2	2
9	M/51	Unknown	29:10 h	17:40 h	4	3	4
10	M/24	Aneurysm	4:50 h	100:10 h	4	3	4
11	F/26	Unknown	9:00 h	12:10 h	3	3	3
12	M/80	Aneurysm	1:10 h	11:10 h	4	4	4
13	F/39	Trauma	1:20 h	104:20 h	4	2	4
14	F/65	AVM	2:10 h	91:20 h	4	4	4
15	M/46	Trauma	3:20 h	98:40 h	4	4	4
16	M/59	Trauma	3:50 h	18:20 h	4	4	4
17	M/26	Trauma	4:00 h	11:00 h	2	2	2
18	M/42	Trauma	2:40 h	27:20 h	4	4	4
19	F/62	Unknown	3:20 h	99:30 h	3	3	3
20	M/34	Unknown	3:00 h	121:50 h	4	4	4
21	M/13	Trauma	1:45 h	21:15 h	4	4	4
22	M/58	Aneurysm	1:20 h	79:40 h	4	4	4
23	M/60	AVM	1:40 h	57:00 h	4	4	4
24	M/79	Unknown	4:20 h	17:45 h	3	3	3
25	F/68	Aneurysm	64:20 h	116:40 h	4	4	4
Mean	48.1		06:18 h	54:16 h	3.4	3.3	3.6

Table 2
SAH in different subarachnoid regions detected by different imaging modalities. SAH detection power of different imaging modalities for each subarachnoid region.

Imaging modality	FPC TD/DO	TOC TD/DO	IHF TD/DO	SVF TD/DO	PMC TD/DO	PFC TD/DO	TNC TD/DO	IVH TD/DO	Total TD/DO	Percent
CT only	20/0	11/0	10/0	15/0	16/0	15/0	8/0	15/0	110/0	75.3/0
FLAIR only	22/1	20/8	13/0	18/1	14/0	16/1	12/0	12/0	127/11	87.0/7.5
SWI only	20/0	12/0	18/2	15/0	15/0	16/1	14/2	19/4	129/9	88.4/6.2
SWI and FLAIR	22/1	21/2	18/6	18/2	16/0	18/1	14/4	19/0	146/16	100/11
SWI and CT	21/0	13/1	18/3	17/1	16/2	17/1	14/0	19/3	135/11	92.5/7.5
CT and FLAIR	22/1	21/1	16/0	18/2	16/1	17/1	12/0	15/0	137/6	93.8/4.1
FLAIR, SWI and CT	22/19	21/9	18/7	18/12	16/13	18/13	14/8	19/12	146/93	100/63.7

Reading example: A total of 21 SAH were found in the temporal-occipital (TOC); FLAIR identified a total of (TD = totally detected) 20 of them, SWI 12, CT 11. By combining SWI and FLAIR all 21 were identified. Combined CT and FLAIR identified 21, and combined SWI and CT identified 13. FLAIR identified 8 SAH (DO = detected only), that were not identified by other modalities.
FPC = frontal-parietal convexity, IHF = interhemispheric cisterns/fissure, IVH = intraventricular hemorrhage), PFC = posterior fossa cisterns, PMC = perimesencephalic cisterns, SVF = Sylvian cisterns/fissure, TNC = tentorial cistern, TOC = temporal-occipital convexity. TD: totally detected; total number of SAHs detected by this (these) modality (-ies). DO: detected only: number of SAHs detected only by this (these) modality (-ies) and not the remaining modality (-ies).

more detailed assessment compared to the usually recommended subdivision into 5 regions [11,12]. The convexity of the subarachnoid spaces was divided into 3 regions: (1) frontal-parietal, (2) temporal-occipital, and (3) interhemispheric fissure; followed by (4) the Sylvian cistern, (5) the perimesencephalic cisterns (combination of mesencephalic cisterns and basal cisterns), (6) posterior fossa cisterns, (7) superior cerebellar cistern (which belongs to the posterior fossa cisterns, but was evaluated separately). Further hemorrhage in the (8) intraventricular space was evaluated.

Intraventricular hemorrhage was separately analyzed and subgrouped into blood in the (1) lateral ventricles, (2) III ventricle and (3) IV ventricle.

CT and MRI findings were interpreted independently by two experienced staff neuroradiologists with at least 10 years experience. Both readers were aware of the diagnosis of SAH, however were blinded to the patients' clinical data and the results of the other imaging techniques. CT, SWI and FLAIR were rated on separate sessions. Main criterion was, whether SAH was detectable or not. If hemorrhage was detected an allocation to the corresponding anatomical region was done. Therefore it was independent of further technical aspects, like 1.5 or 3 T acquisitions. In cases of divergent ratings, consensus reading was established in a final reading session.

Diagnostic interpretation criteria were as follows: in axial non-contrast CT, SAH was diagnosed if an increase of more than 10 Hounsfield units could be measured in the subarachnoid spaces and could be confirmed interactively at the Picture Archiving and Communication System (PACS)-monitor. In the coronal FLAIR images, SAH was diagnosed if a circumscribed signal increase in the CSF space was detected and other reasons for the signal alteration, e.g., flow artifacts, could be excluded. For SWI interpretation we used the standard images without phase images.

If on SWI a non-structurally referenceable hypointense signal alteration was detected in the cisterns, sulci or ventricles, surrounded by iso-intense parenchymal or CSF signal intensity in the subarachnoid space, it was rated as SAH. To differentiate SAH from veins in the sulci, the shape of vessels was evaluated (regular, smooth and uniform versus irregular nonuniform with a rough boundary and a slightly triangular form due to blood content). If hemorrhage was suspected, the neighboring sections were also evaluated to confirm SAH. If CSF was overlaid by susceptibility artifacts due to adjacent bone structures, e.g. in the basilar cisterns, SWI could not ascertain SAH [1,4,7]. Patients with trauma or ruptured AVM who showed parenchymal hemorrhage close to the SAH were excluded of the study to avoid blooming effects. The diagnosis of SAH was set if at least one of the three studied modalities fulfilled the diagnostic criteria mentioned above. Since there was no cross-sectional imaging gold standard for SAH validation, it was not possible to determine whether extra cases of SAH in single modalities were false or true; therefore sensitivity and specificity could not be calculated.

3. Results

A total of 146 regions with SAH were identified by combining CT, FLAIR and SWI (Table 2). Subdivided in regions, 61 (41.8%) of these hemorrhages were interhemispheric, 34 (23.3%) were located in the Sylvian, basal or mesencephalic cisterns, another 32 (21.9%) were seen in the posterior fossa including the superior cerebellar cistern, and 19 (13.0%) were intraventricular.

CT alone identified less SAH (75.3%), than FLAIR (87.0%) or SWI (88.4%). SWI and FLAIR combined detected all identifiable SAH (100%). CT combined with FLAIR detected (93.8%) almost similar percentage of SAH was seen by combining CT with SWI (92.5%). A consensus between all modalities was found in 93 of 146 regions (63.7%) (Table 2). Additional agreements between two modalities (while the third modality disagreed) were found as follows: FLAIR and CT 6 (4.1%), CT and SWI 11 (7.5%), FLAIR and SWI 16 (11.0%). None of the SAH regions was detected by CT only while 7.5% and 6.2% were detected by FLAIR and SWI only, respectively.

FLAIR as single modality identified all SAH in the frontal-parietal sulci (Fig. 1, Table 2) and was more accurate than SWI and CT for the temporo-occipital and sylvian (Fig. 3) regions. SWI detected all interhemispheric SAH (Fig. 2) which was not the case for CT and SWI.

CT was very accurate for perimesencephalic SAH (16 out of 16), followed by SWI (15 out of 16) and FLAIR (14 out of 16) (Fig. 4).

The three modalities were almost equally sensitive for SAH in the posterior fossa cisterns (PFC). SWI outperformed the other techniques in the superior cerebellar cistern (SCC) detecting all 14 cases, while CT and FLAIR detected subarachnoid blood in this region in 8 and 12 cases, respectively. One case must be mentioned separately, since MRI was performed only 2:30 h after symptom onset. SWI showed no typical signal loss in the PMC and PFC, whereas CT and FLAIR clearly showed SAH. However, inhomogeneous signal reduction was seen by SWI in the subarachnoid space. (Fig. 6) This phenomenon was not seen in other patients, where MRI was performed at least 8 h after symptom onset and SWI showed a typical signal loss.

Subdividing the ventricular system into lateral, third and fourth ventricles, a total of 37 intraventricular bleedings were found (Table 3). SWI identified all 37 (100%); CT found 28 (75.7%) and FLAIR 22 (59.5%) intraventricular hemorrhages. See also Fig. 5 as example for the high accuracy of SWI in detecting intraventricular hemorrhage. Further details are listed in Tables 2 and 3. The interrater reliability for the raters was found to be Kappa = 0.877 ($p < 0.001$). In a final session a consensus reading was performed.

Fisher grading was determined for each modality (Table 1) [13]. After performing the sign test we found that there was no

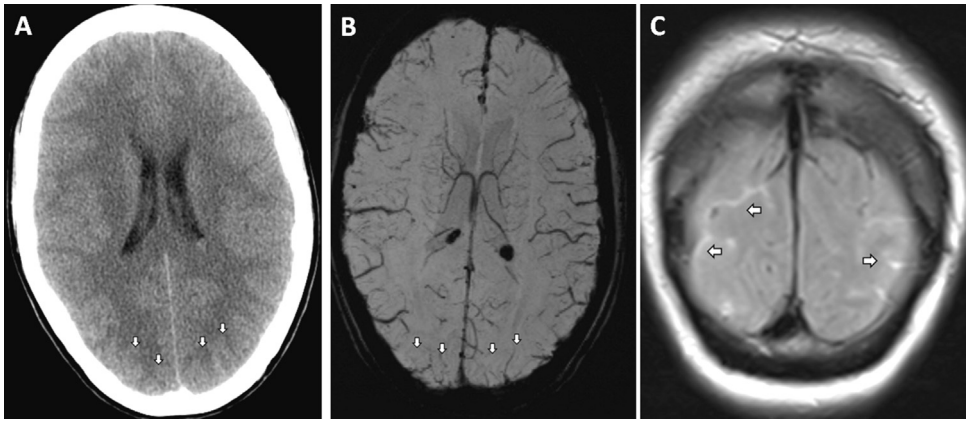

Fig. 1. Temporo-occipital SAH. In transversal CT (A, arrows) and SWI (B, arrows) a temporal-occipital SAH cannot be definitively diagnosed, whereas in the coronal FLAIR sequence, the temporal-occipital SAH is clearly visible (C, arrows); patient no. 11, see Table 1.

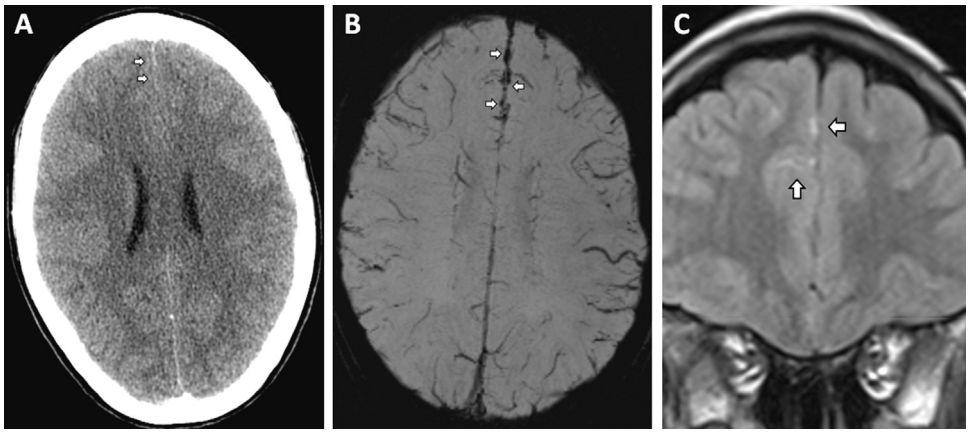

Fig. 2. Fine interhemispheric SAH. In axial CT (A) SAH cannot be diagnosed conclusively, whereas in transversal SWI and coronary FLAIR the fine subarachnoid bleeding can be identified in the interhemispheric cisterns rostrally (C and B; arrows); patient no. 18; see Table 1.

statistically significant difference between each modality. The mean Fisher grade classification for each modality showed no relevant difference. The mean Fisher grade for CT was 3.4, which was between the other two modalities: FLAIR at 3.3 and SWI 3.6.

4. Discussion

Detection of SAH with CT depends on the attenuation values of blood and the individual hemoglobin levels [14–16]. Sensitivity of SAH detection decreases with time with the reduction of hemoglobin concentration. In contrast, signal intensity on FLAIR imaging correlates with cellularity and protein levels, which increase in CSF over time in case of SAH [6,17]. SWI is widely used for detection of parenchymal hemorrhage due to its sensitivity to blood products [9,10,18]. Whereas the sensitivity of CT in detection of SAH is very high within the first 24 h (over 95%), it falls sharply in the following days, FLAIR imaging is reported to be equivalent in the acute phase and even better than CT

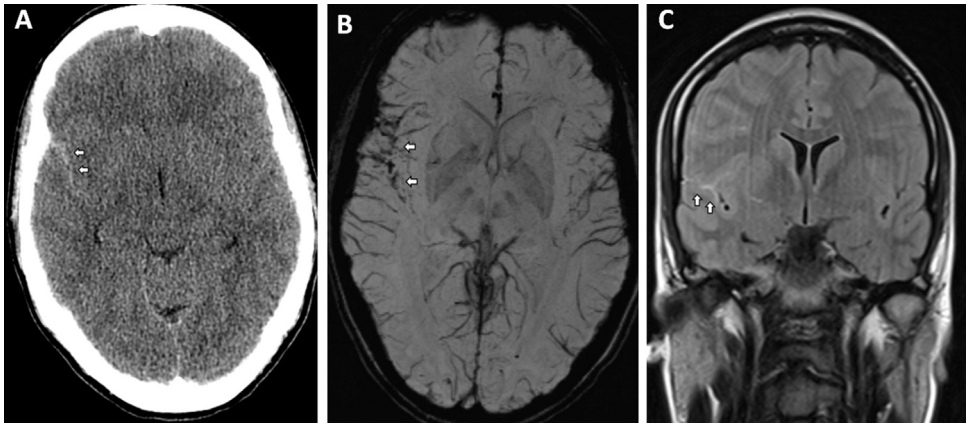

Fig. 3. SAH in sylvian cistern. CT (A) shows SAH in the right sylvian cistern (see arrows). Correspondingly, SAH can be identified clearly by SWI through irregular and nonuniform dark signal intensity in the same location (B). By a hyperintense signal alteration in the sylvian cistern SAH can be identified in FLAIR (C); patient no. 11, see Table 1.

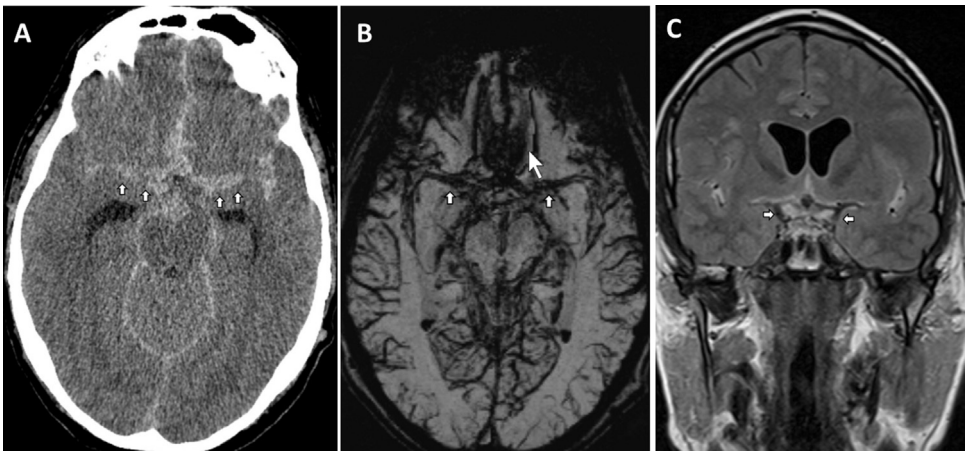

Fig. 4. Perimesencephalic SAH. Perimesencephalic SAH is clearly visible in CT (A, arrows). SWI identifies SAH along the middle cerebral arteries through hypointense irregularities, nonuniform signal and rough vessel boundary (B, small arrows). However, above the sphenoidal sinus it is difficult to differentiate whether the susceptibility artifacts are due to adjacent air and bone structures or due to SAH (B, large arrowhead), while in both CT and FLAIR (C) SAH can be identified distinctly; patient no. 17, see Table 1.

for subacute SAH [2,16,17,19,20]. Unfortunately both imaging techniques lose detection quality over a longer time period. However, as SAH detection in SWI increases with blood decomposition, we expect that detection quality may increase with time.

In this study, SWI and FLAIR detected a higher number of SAH as compared to CT. Comparing CT and FLAIR, these findings are consistent with previous studies that reported FLAIR imaging to be more sensitive for detection of SAH, both in the subacute and acute phases [5,17,19,20]. Detecting SAH with SWI has so far been analyzed in only one study [11]. Our findings are in line with this study by Wu et al., as SWI was sensitive in detecting frontal–parietal, and interhemispheric SAH, as well as intraventricular hemorrhage. The only discrepancy was found in the supracerebellar cistern, where

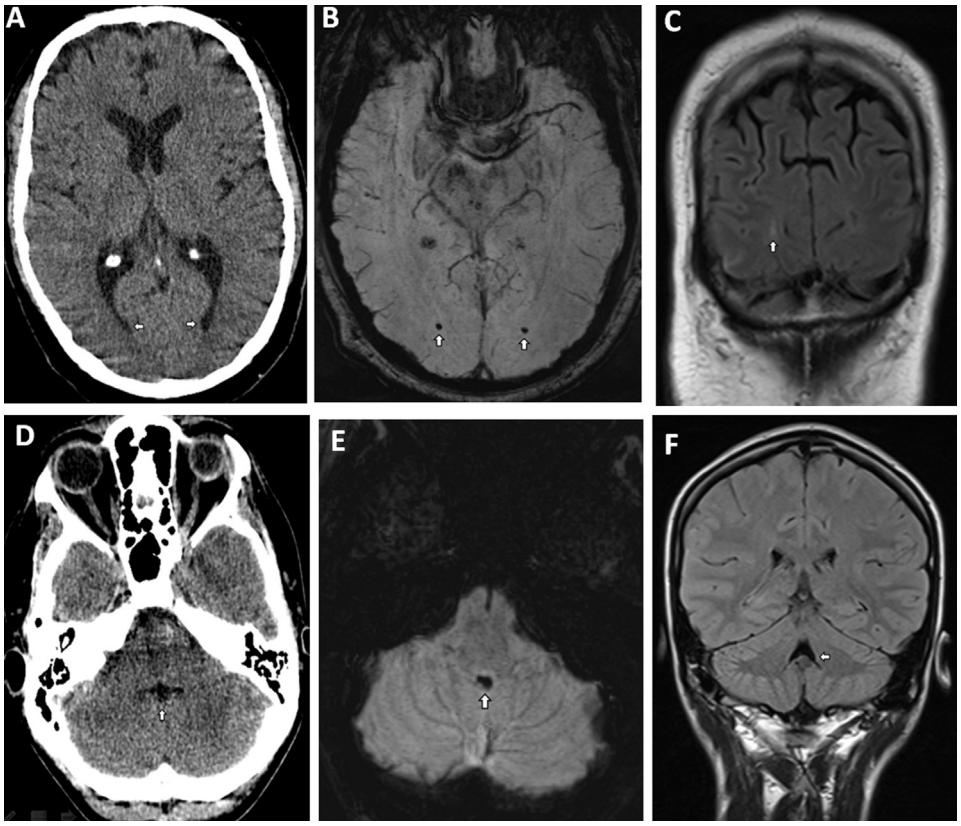

Fig. 5. Intraventricular hemorrhage. In CT (A) no intraventricular hemorrhage can be seen in the posterior horns (arrows), while SWI (B) shows hemorrhage in both posterior horns. FLAIR (C) shows no hyperintense signal on left and slight hyperintense signal on right (arrow), where it is not clear whether it is periventricular (e.g. medullary parenchymal signal alterations) or intraventricular; patient no. 6, see Table 1. In the lower row CT cannot identify SAH in the IV. Ventricle, while SWI (E) shows a signal loss indicating hemorrhage. Again, FLAIR (F) does not show hemorrhage in this ventricle; patient no. 9, see Table 1.

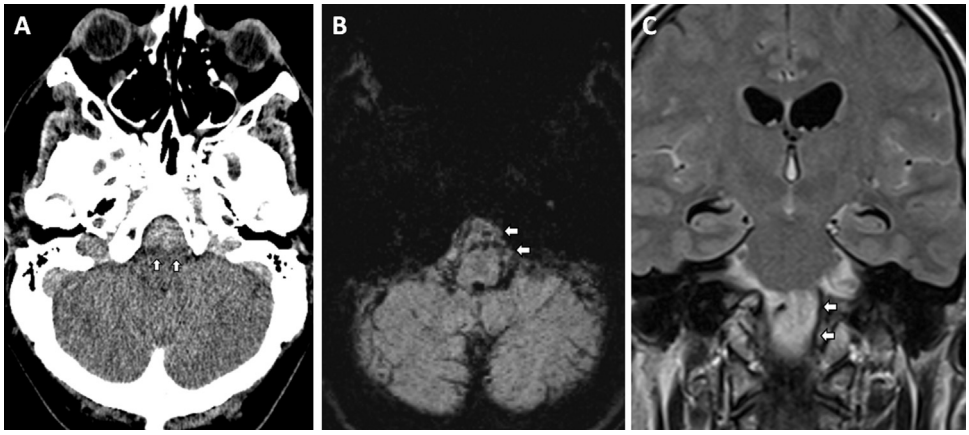

Fig. 6. Perimedullary SAH. In this patient with SAH, MRI was performed only 2.20 h after symptom onset. CT (A) clearly shows a perimedullary SAH. SWI (B) shows at the same location a nearly liquor isointense signal with small mainly linear hypointense irregularities, but not the typical signal loss, mainly due to the lack of time for accumulation of hemosiderin. Correlating to the CT finding FLAIR (C) also has no difficulties in identifying perimedullary SAH; patient no. 1, see Table 1.

our study showed greater sensitivity of SWI as compared to CT. This might be partially explained by the small number of SAH in both patient groups.

All SAHs identified with CT were also identified either by one or both of the two MRI techniques. FLAIR identified 11 (7.5%) SAHs that were not observed in the CT or SWI, of which 8 were in the temporal-occipital cisterns; SWI identified 9 (6.2%) hemorrhages that were not observed in the CT or FLAIR, of which 4 were intraventricular, 2 interhemispheric and 2 supracerebellar. While FLAIR was sensitive in identifying temporal-occipital, frontal-parietal and sylvian SAH, it was relatively insensitive to intraventricular and interhemispheric hemorrhage. CT was sensitive for detection of SAH in the frontal-parietal region, in the Sylvian cistern and the perimesencephalic area, but weaker in the temporal-occipital, interhemispheric, supracerebellar and for intraventricular hemorrhage. A possible explanation for the low performance of FLAIR in detecting intraventricular blood products is the different time-point of image acquisition: MRI was performed at a mean of approximately 48 h after CT, which decreases sensitivity for hemorrhage detection. Furthermore, CSF pulsation regularly occurs in the III and IV ventricle and is often hard to differentiate from intraventricular lesions, which is a well known pitfall in FLAIR imaging. We tended to diagnose “no SAH” if pulsation was not clearly ruled out. CT, on the other hand, missed the smaller hemorrhages, mainly because of beam-hardening artifacts in the posterior fossa and higher partial volume effects (section thickness 1.25–2.5 mm).

The limitations of CT and FLAIR could be partially overcome by the additional use of SWI. SWI was good in identifying interhemispheric and supracerebellar hemorrhage. It identified all 37 intraventricular hemorrhages. This very high detection capacity for intraventricular hemorrhage is consistent with the study of Wu et al. [11], and is partially due to the fact that other sequences are less sensitive for susceptibility effects. In contrast to the subarachnoid spaces, where it might be difficult to differentiate SWI signal decrease due to SAH from normal venous blood, this is no problem in ventricular hemorrhage because subependymal veins can clearly be separated from the ventricular system on SWI. Additionally, since SWI is a high-resolution sequence, even small amounts of hemorrhage can be detected, while partial volume effects are minimal [11]. The areas where SWI was hampered by lower detection rates were the temporal-occipital region and the Sylvian cistern. This may be due to the fact that these areas are closer to the skull or air-filled spaces, and thus are prone to susceptibility artifacts that overlap with the SAH signal.

The combination resulting in the highest detection rate was FLAIR plus SWI, which detected a total of 146 subarachnoid hemorrhages. The principal advantage is their complementary effect, whereas each MRI method alone performed moderately in the perimesencephalic region and in the posterior fossa, but due to their complementary character, all SAHs, including those detected by CT, were identified when their results were combined.

The results highlight the fact that the diagnostic value of the examined modalities depends on the anatomical distribution of the SAH. For the MRI techniques, it seems that FLAIR is sensitive for superficial/convexity SAH, while SWI adds value for the centrally located SAH, e.g. the interhemispheric, supracerebellar and the intraventricular subarachnoid blood. However, SWI has its limitations. SWI does not clearly identify SAH if imaging is performed too early due to short time for hemorrhage decomposition. As shown in this case (Fig. 6), FLAIR compensates for the lack of detection power of SWI. In another case, where acquisition time was 8 h after symptom onset, the typical signal loss of SWI was already present, which implies that extent of blood decomposition is enough for

Table 3
IVH detection in the different regions of the ventricular system by different imaging modalities.

Imaging modality	III ventricle TD/DO	IV ventricle TD/DO	Lat. ventricle TD/DO	Total TD/DO	Percent TD/DO
CT only	7/0	8/0	13/0	28/0	75.7/0
FLAIR only	6/0	4/0	12/0	22/0	59.5/0
SWI only	8/0	12/4	17/3	37/7	100/18.9
SWI and FLAIR	8/1	12/0	17/1	37/2	100/5.4
SWI and CT	8/2	12/4	17/2	37/8	100/21.6
CT and FLAIR	8/0	8/0	14/0	30/0	81.1/0
FLAIR, SWI and CT	8/5	12/4	17/11	37/20	100/54.1

TD: totally detected; total number of SAHs detected by this (these) modality (-ies). DO: detected only: number of SAHs detected only by this (these) modality (-ies) and not the remaining modality (-ies).

susceptibility effects after that period. A further diagnostic pitfall can be the presence of calcifications. Though calcification and hemorrhage both show a signal loss in SWI, the differentiation is possible not only by shape and typical localization, but also by analyzing the corresponding signal in FLAIR sequence, which is hypointense for calcification and hyperintense for SAH.

Fisher score, as a grading system for SAH and prognostic tool for the development of vasospasm, did not differ considerably between the 3 imaging modalities, suggesting that this classification can be used in all modalities.

MRI has certain disadvantages compared to CT. Especially in trauma patients, a clear evaluation of bone fractures is indispensable; here, CT has a much higher sensitivity than MRI. Furthermore CT is widely available, rapidly acquired, cost-effective und uncomplicated to perform, especially in very ill, e.g., intubated patients. The availability of MRI is limited, and the examination of these acutely ill patients is intensive with regard to time and staff. On the other hand, MRI offers additional information, e.g., shearing injuries, edema, or other potential sources of SAH, e.g., AVM. Therefore, the benefits and costs of MRI versus CT need to be decided on an individual basis.

Similar to previous investigations [11], this study has several limitations. It is a retrospective study with a rather limited number of SAH patients, which received both CT and MRI. The latter can be explained by the fact that scanning such patients with both CT and MRI is rather the exception in our institution. CT remains the workhorse for such indications. CT and MRI scans were often not acquired on the same day obviously due to logistic considerations, since these are critically ill patients managed in the intensive care unit. FLAIR scans had a coronal orientation in accordance with our routine cranial MRI protocol, and had to be compared to axial CT and SWI images. Furthermore, there was no gold standard for confirmation of the SAH.

In summary, this study demonstrates that a combination of SWI and FLAIR yields a distinctly higher detection rate for SAH due to their complementary detection capabilities. The detection strength of SWI is high for centrally located hemorrhages, i.e., intraventricular and interhemispheric. FLAIR, on the other hand, provides excellent detection of superficial SAH. The frequency of undetected SAH was the highest for CT. This study suggests, that if MRI is planned for a suspected SAH, then a combination of FLAIR and SWI has to be included whenever possible.

Conflict of interest

We declare that we have no conflict of interest.

References

[1] Provenzale JM, Hacein-Bey LCT. evaluation of subarachnoid hemorrhage: a practical review for the radiologist interpreting emergency room studies. Emergency Radiology 2009;16:441–51.
[2] van Gijn J, Kerr RS, Rinkel GJ. Subarachnoid haemorrhage. Lancet 2007;369:306–18.
[3] da Rocha AJ, da Silva CJ, Gama HP, et al. Comparison of magnetic resonance imaging sequences with computed tomography to detect low-grade subarachnoid hemorrhage: Role of fluid-attenuated inversion recovery sequence. Journal of Computer Assisted Tomography 2006;30:295–303.
[4] Shimoda M, Hoshikawa K, Shiramizu H, et al. Problems with diagnosis by fluid-attenuated inversion recovery magnetic resonance imaging in patients with acute aneurysmal subarachnoid hemorrhage. Neurologia Medico-Chirurgica 2010;50:530–7.
[5] Noguchi K, Ogawa T, Inugami A, et al. Acute subarachnoid hemorrhage: MR imaging with fluid-attenuated inversion recovery pulse sequences. Radiology 1995;196:773–7.
[6] Stuckey SL, Goh TD, Heffernan T, et al. Hyperintensity in the subarachnoid space on FLAIR MRI. American Journal of Roentgenology 2007;189:913–21.
[7] Mostrom U, Ytterbergh C. Artifacts in computed tomography of the posterior fossa: a comparative phantom study. Journal of Computer Assisted Tomography 1986;10:560–6.
[8] Haacke EM, Xu Y, Cheng YC, et al. Susceptibility weighted imaging (SWI). Magnetic Resonance in Medicine 2004;52:612–8.
[9] Sehgal V, Delproposto Z, Haacke EM, et al. Clinical applications of neuroimaging with susceptibility-weighted imaging. Journal of Magnetic Resonance Imaging 2005;22:439–50.
[10] Santhosh K, Kesavadas C, Thomas B, et al. Susceptibility weighted imaging: a new tool in magnetic resonance imaging of stroke. Clinical Radiology 2009;64:74–83.
[11] Wu Z, Li S, Lei J, et al. Evaluation of traumatic subarachnoid hemorrhage using susceptibility-weighted imaging. American Journal of Neuroradiology 2010;31:1302–10.
[12] Osborn AG, Tong KA. Handbook of neuroradiology: brain and skull. 2nd ed. St. Louis: Mosby; 1996. p. 25.
[13] Claassen J, Bernardini GL, Kreiter K, et al. Effect of cisternal and ventricular blood on risk of delayed cerebral ischemia after subarachnoid hemorrhage: the Fisher scale revisited. Stroke 2001;32:2012–20.
[14] Norman D, Price D, Boyd D, et al. Quantitative aspects of computed tomography of the blood and cerebrospinal fluid. Radiology 1977;123:335–8.
[15] Fainardi E, Chieregato A, Antonelli V, et al. Time course of CT evolution in traumatic subarachnoid haemorrhage: a study of 141 patients. Acta Neurochirurgica 2004;146:257–63 [discussion 63].
[16] Sames TA, Storrow AB, Finkelstein JA, et al. Sensitivity of new-generation computed tomography in subarachnoid hemorrhage. Academic Emergency Medicine 1996;3:16–20.
[17] Maeda M, Yagishita A, Yamamoto T, et al. Abnormal hyperintensity within the subarachnoid space evaluated by fluid-attenuated inversion-recovery MR imaging: a spectrum of central nervous system diseases. European Radiology 2003;13(Suppl. 4):L192–201.
[18] Haacke EM, Mittal S, Wu Z, et al. Susceptibility-weighted imaging: technical aspects and clinical applications, part 1. American Journal of Neuroradiology 2009;30:19–30.
[19] Mitchell P, Wilkinson ID, Hoggard N, et al. Detection of subarachnoid haemorrhage with magnetic resonance imaging. Journal of Neurology, Neurosurgery and Psychiatry 2001;70:205–11.
[20] Noguchi K, Ogawa T, Seto H, et al. Subacute and chronic subarachnoid hemorrhage: diagnosis with fluid-attenuated inversion-recovery MR imaging. Radiology 1997;203:257–62.